Journal of Applied Polymer Science

Effect of Five Saturated Fatty Acids on the Properties of Sweet-Potato-Starch-Based Films

Pengfei Liu, Shenglin Sun, Hanxue Hou, Wentao Wang, Haizhou Dong
Department of Food Science and Engineering, Shandong Agricultural University, Tai'an 271018, People's Republic of China
P. Liu and S. Sun contributed equally to this article.
Correspondence to: H. Dong (E-mail: haizhoudong@126.com)

ABSTRACT: To fully explore the influences of saturated fatty acids (SFAs) on the properties of sweet-potato-starch (SPS)-based films, five SFAs were chosen to add to SPS. The SPS-based films were prepared by casting. The microstructure, mechanical, optical, water vapor barrier, and thermal properties of the films were investigated. The 2.0% (w/w, on the basis of starch) SFA significantly changed the SPS pasting characteristics in the peak viscosity, breakdown, and other feature point viscosity values as determined by a Rapid Visco Analyser. The amylose molecular weights decreased as measured by high-performance size exclusion chromatography. A thermal study with differential scanning calorimetry suggested that the addition of SFA increased the onset temperature and peak temperature. Scanning electronic microscope (SEM) images showed a continuous and uniform structure in the films with SFA. The SPS–SFA composite films showed lower light transmission and elongation at break than the control. Compared with the control films, the addition of SFA increased the tensile strength and decreased the water vapor permeability of the films. © 2014 Wiley Periodicals, Inc. J. Appl. Polym. Sci. **2015**, *132*, 41380.

KEYWORDS: biodegradable; biomaterials; biopolymers and renewable polymers

Received 21 May 2014; accepted 4 August 2014
DOI: 10.1002/app.41380

INTRODUCTION

In view of the severe environmental pollution caused by plastic food packaging, the interest in edible and biodegradable films made from natural polymers and the need for environmentally friendly polymers has increased. Among natural polymers, starch is one of the most promising candidates for preparing biodegradable films because it is a renewable source and is widely available, abundant, relatively easy to handle, and inexpensive.[1,2]

Sweet potatoes are widely cultured in China, which has the highest production in the world.[3] Because of storage difficulties and inefficient processing, up to 15% of their sweet potatoes are discarded every year.[4] Because sweet potatoes are an edible and biodegradable material, the preparation of sweet-potato-starch (SPS)-based films is a good way to reduce this waste. Starch-based films have been widely studied; these include corn-, potato-, and tapioca-starch-based films,[5–7] whereas study on SPS-based films is relatively scarce. The poor mechanical properties of SPS-based materials hinder their extensive use. In addition, the highly hydrophilic nature of SPS is another major limitation that seriously restricts the development of SPS-based polymer matrices. They are sensitive to water and absorb water easily in a high-humidity environment.[8] The polymer matrix shows poor moisture barrier properties; this is a critical issue for various commercial applications.

To expand the application of SPS-based films, it is necessary to reduce their hygroscopicity. Fatty acids, which are known to exhibit good hydrophobic properties, have been incorporated into the polymer matrix to reduce their water vapor permeability (WVP).[9] Gontard et al.[10] reported that lipids could cause a decrease in the WVP of biopolymer films. Several studies have also used fatty acids to reduce the hygroscopic properties of the polymer matrix and to improve the WVP.[11–13]

At present, the effects of saturated fatty acids (SFA) on the properties of SPS and SPS-based films have not been reported, and some questions remain unclear concerning the effect of fatty acids on the properties of starch-based films. For instance, is there a relation between the mechanical properties and WVP properties and the carbon chain length of the fatty acids? Does the addition of fatty acids increase or decrease the tensile strength (TS) values of the films?

The objective of this research was to develop films based on SPS with the addition of 33% glycerol (GLY; w/w, on the basis of SPS) as a plasticizer and the addition of different SFAs [arachidic acid (AA), stearic acid (SA), palmitic acid (PA),

myristic acid (MA), and lauric acid (LA)] to improve their properties. Another aim of this study was to further investigate the interaction between amylose molecules and SFA molecules. In addition, the effects of SFAs of different carbon chain lengths on the pasting properties and the molecular weight (MW) distribution of SPS and on the thermal, microstructure, mechanical, optical and WVP properties of SPS–SFA composite films were studied.

EXPERIMENTAL

Materials

SPS was provided by Rushan Huamei Starch Products Co., Ltd. (Weihai, China). Gly was obtained from Kaitong Chemical Reagent Co., Ltd. (Tianjin, China). AA, SA, PA, MA, and LA were purchased from Yuanye Biotechnology Co., Ltd. (Shanghai, China).

Addition of the SFAs

SFA solutions were prepared by the dissolution of 120 mg of SFA (AA, SA, PA, MA, and LA) in 60 mL of absolute ethanol. SPS (6.0 g) was added to each of the SFA solutions. The mixtures were gently shaken in an Accura Te Strengthen Electronic Stirrer (Guohua Electrical Equipment Co., Ltd., Changzhou, China) at 60°C for 120 min, and then, the solvents were evaporated in a vacuum-drying oven (Jinghong Laboratory Instrument Co., Ltd., Shanghai, China) at 50°C. The dried samples were then ground into a fine powder for further experiments. The SPS without SFA addition was used as the control sample.

Effect of SFA on the Pasting Properties of SPS

The pasting properties of the SPS samples were determined with a SUPER-3 Rapid Visco Analyser (Newport Scientific Instruments Co., Australia). The viscosity was expressed in rapid viscosity units (RVUs). The samples with or without SFA (2.5 g) were slurried with distilled water (25 mL). The sample was stirred at high speed (960 rpm) for 10 s to disperse the sample, and then, the speed was maintained at 160 rpm during the process. The sample was held at 50°C for 1 min, then heated up to 95°C for 3.7 min, and held at 95°C for 2.5 min. The sample was then cooled to 50°C within 3.8 min and held at 50°C for 2 min.

The Rapid Visco Analyser provided the following parameters: peak viscosity (PV), or the highest viscosity; trough viscosity (TV), or the lowest viscosity; breakdown (BD; BD = PV − TV); final viscosity (FV), or the viscosity at the completion of the cycle; and setback (SB; SB = FV − TV).[14]

Effect of the SFAs on the MW Distribution of SPS

Preparation with Wet Methods. The SPS–SFA and the control sample without SFA (150 mg) were combined with aqueous dimethyl sulfoxide (15 mL; 90:10) and was stirred at 96°C for 60 min. Then, they were cooled to room temperature and stirred for 24 h. The mixture (5 mL) was added to 25 mL of anhydrous ethanol and then equilibrated for 10 min. The mixture was centrifuged at 4000 × g for 15 min. The acquired precipitates were then washed with 95% ethanol and centrifuged again at 4000 × g for 2 min. Then, 10 mL of water was added to the precipitate, stirred at 100°C for 30 min, and then filtered with a 5-μm syringe-driven filter to obtain the liquid, which was used for further analysis.

Measurement of MW. The MW was measured with a high-performance size exclusion chromatography instrument (Shimadzu Inc., Kyoto, Japan) equipped with an autosampler and a single-detector system, a refractive index detector (RID-10A). The TSK gel G4000PWXL, G5000PWXL column (7.8 mm *i.d.* × 300 mm per column) with a TSK guard column (4.6 mm *i.d.* × 35 mm; Tosohaas Co., Ltd., Tokyo, Japan). The column temperature was maintained at 60°C. A sodium nitrate solution (0.3 mol of $NaNO_3$) containing 0.2 g/kg of sodium azide (NaN_3) was used as the mobile phase at a flow rate of 0.5 mL/min. The injection volume of the samples was 10 μL.

Preparation of the Films

The SPS–SFA specimen powders (containing 6 g of SPS and 120 mg of SFA) were dispersed into distilled water (200 mL), and 33% Gly (w/w, on the basis of SPS) was then added. The film-forming suspension was heated in a water bath at 90°C for 90 min through continuous mixing with the Accura Te Strengthen Electronic Stirrer (Guohua Electrical equipment Co., Ltd., Changzhou, China) at 350 rpm. The solution was homogenized with an IKA T18 basic Ultra-Turrax (Germany) at 14,000 rpm for 4 min. The obtained solutions were filtered through the gauze. A film-forming suspension was poured on 120 × 240 mm^2 Teflon-coated glass plates. The SPS-based films were obtained by the evaporation of water in a vacuum-drying oven at 40°C. The films were obtained by peeling from the Teflon-coated glass plates. The control sample was also used to prepare films in the same way.

All of the tested samples were equilibrated at 23 ± 2°C and 53% relative humidity in a constant-temperature and constant-humidity chamber (Jinghong Experimental Equipment Co., Ltd., Shanghai, China) for at least 2 days before testing.

Light Transmission

The visible light barrier properties of the films were determined in a wavelength range from 400 to 800 nm with a T6 New Century ultraviolet spectrophotometer (model UV-2100, Pgeneral Instrument Co., Ltd., Beijing, China). The SPS–SFA composite films and the control films were cut to 5 × 1 cm^2 before testing. The light transmission values of the composite films and the control films were calculated according to the following equation:

$$\text{Light transmission} = 10^{-A_{400-800}} \quad (1)$$

where $A_{400-800}$ is the absorbance at 400–800 nm.

Mechanical Properties of Films

The mechanical properties of the composite films and the control films were determined with tension tests with a TA-XT2i texture analyzer (Stable Micro System Co., United Kingdom) according to ASTM D 882-02.[15] They were cut into strips (15 × 100 mm^2) with a sharp knife. The initial distance between the grips was 50 mm, and the test speed was 1 mm/s. TS (MPa) and elongation at break (*E;* %) were calculated by six replicates on the basis of previous studies:[16]

Table I. Effects of SFAs on the Pasting Properties of SPS

Sample	PV (RVU)	TV (RVU)	BD (RVU)	FV (RVU)	SB (RVU)
Control	295.8 ± 3.9	181.6 ± 5.8	114.2 ± 9.6	260.1 ± 10.4	78.5 ± 4.7
SPS-AA	282.4 ± 3.9	177.5 ± 3.6	104.9 ± 5.0	263.7 ± 8.1	86.2 ± 9.6
SPS-SA	275.1 ± 4.6	193.2 ± 4.3	81.9 ± 2.1	251.7 ± 4.4	58.5 ± 2.0
SPS-PA	275.8 ± 5.3	179.1 ± 1.2	96.7 ± 6.2	256.3 ± 9.6	77.2 ± 9.8
SPS-MA	247.2 ± 1.9	200.1 ± 5.9	47.1 ± 4.0	246.1 ± 5.1	46.0 ± 7.1
SPS-LA	256.7 ± 5.5	198.0 ± 9.9	58.7 ± 4.4	263.6 ± 5.8	65.6 ± 9.0

$$\text{TS} = L_P/A \times 10^{-6}\text{MPa} \quad (2)$$

where L_P is the peak load (N) and A is the cross-sectional area of the films (m^2).

$$E = \Delta L/L \times 100\% \quad (3)$$

where ΔL is the increase in the length at the breaking point (mm) and L is the original length of the samples (mm).

WVP

The WVP of the composite films and the control films were determined with a water vapor transmission rate tester (PERME W3/030, Labthink Instruments Co., Ltd., China). The films should have remained smooth, without wear and breakage. The films were cut into round shapes (33.00 cm^2) with a special sampler. The relative humidity and temperature for testing were 90% and 38°C, respectively. The WVP of each sample was averaged from three separate tests:[17]

$$\text{WVP} = \Delta m \times d/(A \times t \times \Delta p) \quad (4)$$

where Δm is the increment of the quality (g), d is the thickness of the sample (cm), A is the area of the sample (cm^2), t is the interval time (s), and Δp is the vapor pressure differential across the film (Pa).

Differential Scanning Calorimetry (DSC)

The transition temperatures [i.e., onset temperature (T_o) and peak temperature (T_p)] of the SPS–SFA composite films and the control films were measured with a DSC 200PC (Netzsch Scientific Instruments, Germany). Calibration was done on the basis of pure indium, bismuth, stannum, and zinc. Then, 5-mg samples were weighed in aluminum pans and hermetically sealed. The samples were scanned at a rate of 10°C/min in the temperature range from −50 to 250°C for 30 min. The DSC cell was flushed with liquid nitrogen at a flow rate of 20 mL/min to maintain a stable environment.[18]

Scanning Electron Microscopy (SEM)

SEM analysis was made on a Supra 55 (ZEISS, Germany) electron microscope at an accelerating voltage of 5 kV. All of the samples adhered to a conductive carbon tape and were sputter-coated with Au/Pd.

RESULTS AND DISCUSSION

Pasting Properties

Pasting properties are known as one of the most important parameters in the evaluation of starch properties.[19] The effects of the SFAs on pasting properties of SPS are shown in Table I. The SPS with SFA had significantly decreased PV and BD values, and other feature point viscosity values were decreased compared with those of the control samples (Table I). The decrease in PV indicated that the presence of SFA effectively hindered the hydration and swelling behaviors of starch granules during gelatinization. Previous studies suggested that SFAs may cover the granular surface of starch, increasing its hydrophobicity and inhibiting water transfer into the starch granules.[20] The obtained BD values demonstrated that the SPS granules with SFAs showed greater resistance to hydrothermal disruption during gelatinization.[19] Similar results were also observed by other authors.[21]

Some researchers suggested that fatty acids affect the pasting process by either promoting or retarding gelatinization; this depends on the carbon chain length of the fatty acids.[22] Our work further indicated that the pasting properties of the SPS were greatly affected by the carbon chain length of the SFAs. Compared with the control, the starches containing AA (C20:0), SA (C18:0), and PA (C16:0), which had longer carbon chains showed decreases in PV and BD of 4.5–7.0 and 8.1–28.3%, respectively. On the other hand, for the starches containing MA (C14:0) and LA (C12:0), which had shorter carbon chains, the PV and BD decreased 13.2–16.4 and 48.6–58.8%, respectively. This behavior could be explained by the fact that MA and LA had relatively shorter carbon chains than all of the SFAs used; this facilitated their incorporation into the starch and gave greater resistance to hydrothermal disruption during gelatinization.

MW Distribution

Starch consists of two main homopolysaccharides, amylose and amylopectin, which are based on chains of 1→4 linked *a*-D-glucopyranose. Amylose is essentially linear, whereas amylopectin is

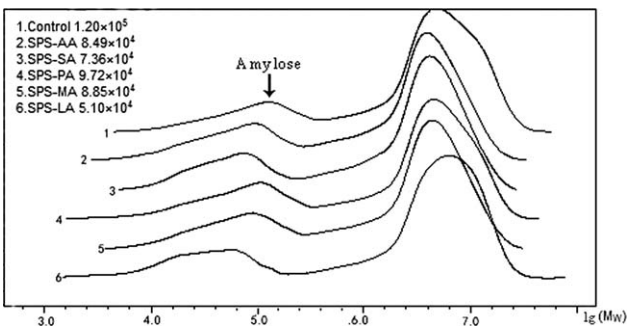

Figure 1. Effects of SFAs on the MW distribution of SPS.

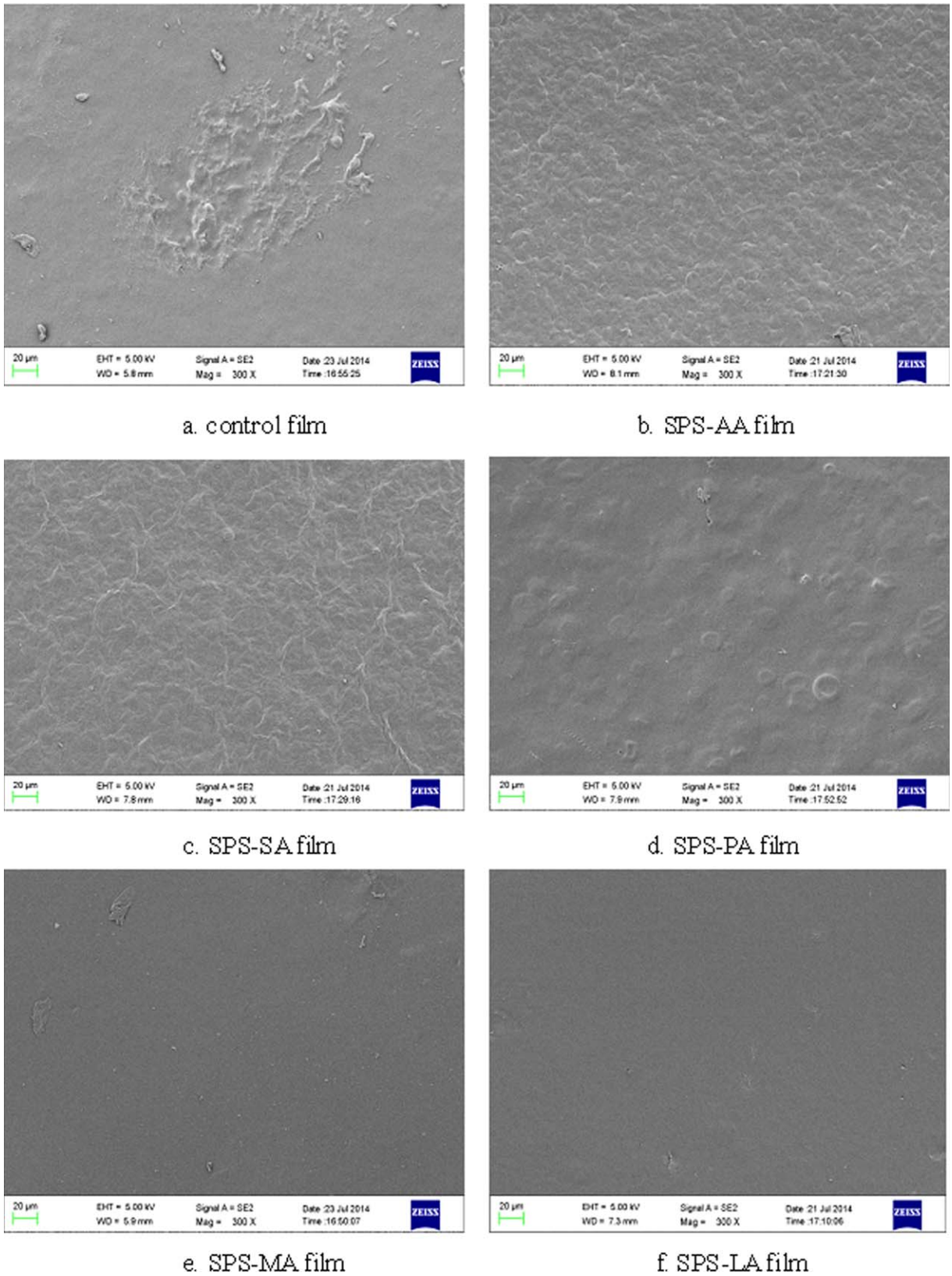

Figure 2. SEM micrographs of the SPS SFA composite films. [Color figure can be viewed in the online issue, which is available at wileyonlinelibrary.com.]

Table II. Effects of the SFAs on the Mechanical Properties of the Films

Film	TS (MPa)	*E* (%)
Control	5.103 ± 0.261	11.877 ± 0.625
SPS–AA	5.842 ± 0.243	7.107 ± 0.757
SPS–SA	5.603 ± 0.317	7.660 ± 0.521
SPS–PA	5.386 ± 0.268	8.427 ± 0.622
SPS–MA	6.327 ± 0.276	7.189 ± 0.382
SPS–LA	6.713 ± 0.155	6.781 ± 0.778

highly branched because of its 1→6 glycosidic bonds.[23] Figure 1 shows the effect of SFA on the MW distribution of SPS. The range of MW values of amylose by different types of SFAs was from 5.10×10^4 to 9.72×10^4 compared with the control sample, which had an MW of 1.20×10^5. The addition of SFAs lowered the MW values of amylose; this could be ascribed to the formation of amylose–lipid complexes.[21,24] Some researchers have reported that amylose–lipid complexes form during the addition of lipids.[25] Amylose is unique among polymers because it has the ability to interact with polar compounds, such as fatty acids, and form helical inclusion complexes.[26] Hydrophobic complexing agents can lie inside of the amylose helix, which is stabilized through van der Waal's interactions through contact with the adjacent C hydrogens of amylose.[27] When starch granules are heated up to the gelatinization temperature in water, the granules swell because of loss of the crystalline order and the absorption of water.[28] At the same time, the amylose inside the starch granules is leached out and forms amylose–lipid complexes with the SFAs. The carbon chain end of the lipids is located in the helix of amylose molecules, and this combination mode eventually leads to the formation of inclusion complexes.[29] So, the MW values of amylose decreased compared with that of the control as the SFAs were added; this was similar to results reported by other researchers.[19]

Our study also showed that the MW distribution of SPS was greatly influenced by the SFA category. The SPS–LA (C12:0) sample had the lowest MW values of amylose compared to the others. This behavior could be explained by the fact that amylose molecules with shorter chains were more easily leached out of the starch granules and readily interacted with the LA, which had the shortest carbon chain length among the five SFAs.[30] In addition, the amylose molecules had a helical conformation, and the LA molecules easily occupied the helical cavity, which had stronger interactions with the amylose molecules than the other SFAs.[31]

SEM Observations

Figure 2 shows the microstructure of the SPS–SFA composite films and the control film. It was obvious that the control films showed an irregular ridged structure and discontinuous matrix; this indicated poor mechanical properties [Figure 2(a)]. Figure 2(b–f) shows the SEM photos of the SPS–SFA composite films. Compared with the control, the composite films exhibited a continuous and uniform structure. The surfaces of the SPS–LA/MA composite films were smooth, whereas the SPS–AA/SA/PA films were rough. This indicated that LA and MA were more compatible with the SPS matrix. In addition, the films with LA (C12:0) and MA (C14:0), which had shorter carbon chains, showed uniform and compact matrices without apparent starch granules, and this was a good indicator of the integrity of the films' structures. It indicated that good mechanical properties of the films with LA (C12:0) and MA (C14:0) would be expected, as obtained in the mechanical tests. On the other hand, the incorporation of SFAs with longer carbon chains (up 14 carbon atoms) seemed to have little effect on the continuity of the films compared with the SPS–LA/MA films.

Mechanical Properties

Table II shows the results of the mechanical tests in terms of the TS and *E* values of the films. The results indicate that the addition of SFAs was able to affect the mechanical properties of the polymer matrix. They show that 2% SFA added to the SPS improved the TS of the films but lowered *E*. Compared with the control film, the TS of the SPS–SFA films showed an increase of 5.5–31.6% and a decrease of 29.1–42.9% in *E* (Table II). This may have been due to the effective, uniform incorporation of SFA in the SPS matrix, which led to an increase in the network resistance. Furthermore, all of the SFAs had a hydrophobic carbon chain at one end of molecules; this could have reduced the moisture content of the films. A low moisture content increased the brittleness of the films, and this led to the decrease in *E*. Meanwhile, as the moisture content decreased, the films became more rigid, and this led to the increase in the TS. A similar result was observed by other researchers.[32]

The films with LA (C12:0) and MA (C14:0), which had shorter carbon chains, showed relatively higher TS values than the films with PA, SA, and AA. This suggested that SPS had good compatibility with shorter chain SFAs. LA and MA had shorter carbon chains, which caused their hydrophilicity to be small and allowed for stronger interactions with other ingredients present in the polymer matrix. Furthermore, their small size allowed them to be inserted into the polymer chains and gave greater strength to the composite films.[23] On the other hand, the AA (C20:0), SA (C18:0), and PA (C16:0), which had longer carbon chains, hindered the formation of the films during processing, and fragile regions emerged. Contrary to this result, Shellhammer and Krochta[33] reported that the TS of the protein–lipid films showed a decreasing trend with the addition of fatty acids. Jimenez et al.[13] studied the effect of the addition of lipids on hydroxypropyl methylcellulose (HPMC) edible films. Their results show that the addition of fatty acids had a negative effect on the mechanical properties. Therefore, the effect mechanism of SFA on the mechanical properties of starch-based films should be studied further.

DSC

DSC is a common method used for the investigation of the thermal properties of starch-based films. Table III shows the T_o and T_p values of the SPS–SFA composite films and the control films. The T_o and T_p values were very close for both the control film and the SPS–SFA composite films; this indicated that the polymer matrix mostly melted and lost its structure when it was used in sealing.[34] The range between T_o and T_p of the control films was broader than those of the SPS–SFA composite films. So, we concluded that SFA had a negative effect on the

Table III. Effects of the SFAs on the Thermal Properties of the Films

Film	T_o (°C)	T_p (°C)	$T_p - T_o$ (°C)
Control	175.7 ± 2.09	182.7 ± 1.58	7
SPS-AA	185.9 ± 1.72	190.2 ± 1.26	4.3
SPS-SA	184.5 ± 1.87	190.8 ± 0.96	6.3
SPS-PA	185.1 ± 2.17	191.8 ± 1.47	6.7
SPS-MA	179.7 ± 1.92	184.3 ± 1.58	4.6
SPS-LA	179.4 ± 1.81	185.5 ± 2.32	6.1

heat sealability of the SPS-based films. The SPS–PA composite film had a relatively broader range in T_p and T_o than the other films (excluding the control ones). SFA addition produced increases in the T_o and T_p values. The results may have been caused by the amylose–lipid complex formation and the strong molecular interaction between the SPS molecules and SFAs. The thermal decomposition temperature of native starch was lower than the melting temperature. So, the native starch had no melting processes through heat treatment. The SPS should be modified and processed to acquire the ideal thermoplastic properties.

Light Transmission

The light transmission was greatly related to the film's function because of their great impact on the appearance of the coated products.[35] The different light transmission of the films was connected with their internal structure developed during film drying.[36] The effects of the SFAs on the light transmission of the SPS–SFA composite films and the control films are shown in Table IV, where the values of light transmission at 400–800 nm are shown for all of the films. The SFA-free films exhibited the greatest light transmission, whereas the presence of SFAs increased the film opacity. This may have been due to the SFA covering the starch granular surface and increasing its compactness. In addition, the formation of the amylose-lipids complex may have been associated with the enhancement of the starch granule structure, which impacted light penetration into the film matrix. The effects of the SFAs on the light transmission of the films were in agreement with those obtained by other researchers.[37,38]

Over the wavelength range (400–800 nm) considered, a similar trend was observed for all of the composite films. The light transmission in the visible region increased with increasing wavelength for all of the samples. The type of SFA greatly affected the light transmission values at a constant wavelength. With increasing number of carbon chains (from C12:0 to C20:0), the light transmission values of the films gradually increased. The films containing LA (C12:0) and MA (C14:0), which had shorter carbon chains, had lower light transmission values compared with the films with SFAs with longer carbon chains. This behavior could be explained by their small size, which allowed them to be inserted into the polymer chains more easily than the longer chain SFAs; this made the polymer matrix more compact. So, their compact network structure impeded the light penetration into the starch films.

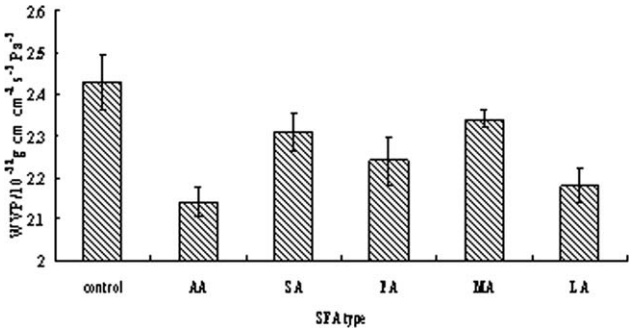

Figure 3. Effects of the SFAs on the WVP of the films.

WVP

Figure 3 shows the WVPs of the SPS-based films (with and without SFAs) analyzed at 23 ± 2°C and 53% relative humidity. The addition of SFAs reduced the WVP values compared with those of the SFA-free films. The values of WVP ranged from 2.14×10^{-12} to 2.34×10^{-12} g cm cm^{-2} s^{-1} Pa^{-1} for the SPS–SFA composite films compared with the control film, for which the value of WVP was 2.43×10^{-12} g cm cm^{-2} s^{-1} Pa^{-1}. This was attributed to the hydrophobicity of the SFA present in the film composition.[39] The SFA may have covered the SPS granular surface and increased its hydrophobicity, and this influenced water transference into the granules.[20] This was consistent with a previous report by Nobrega et al.,[23] who studied cassava-based films. Jiménez et al.[13] reported that the samples containing SA showed a decrease of 26.6% in WVP compared with the pure films. Sanchez et al.[40] studied the effects of lipid materials on the water barrier properties of the HPMC matrix. They found that the water barrier properties

Table IV. Effects of the SFAs on the Light Transmission of the Films

	Light transmission (%)				
Film	400-nm wavelength	500-nm wavelength	600-nm wavelength	700-nm wavelength	800-nm wavelength
Control	78.2 ± 1.27	81.4 ± 1.13	83.2 ± 0.78	85.4 ± 0.57	86.5 ± 0.21
SPS-AA	75.4 ± 1.13	79.1 ± 1.06	81.1 ± 0.92	82.4 ± 0.85	83.5 ± 0.64
SPS-SA	74.3 ± 0.28	76.8 ± 0.14	78.2 ± 0.21	78.8 ± 0.42	79.6 ± 0.35
SPS-PA	73.6 ± 0.71	76.1 ± 0.49	77.6 ± 0.42	78.3 ± 0.35	79.2 ± 0.28
SPS-MA	68.5 ± 1.13	71.8 ± 0.85	73.1 ± 0.42	74.5 ± 0.49	75.7 ± 0.21
SPS-LA	67.6 ± 0.64	70.6 ± 0.42	72.1 ± 0.35	73.2 ± 0.28	74.1 ± 0.21

were improved when lipids were added to the HPMC matrix. PA and SA were found to be effective in reducing the moisture absorption of the Zein sheets.[41] Contrary to these results, Pascat[42] reported that films with PA showed a relatively higher WVP than native films.

Figure 3 also shows the different WVPs of the SPS–SFA composite films. Some authors have claimed that the WVP value decreased with increasing chain length of fatty acids.[43,44] Nevertheless, some researchers also observed that the moisture permeability increased as the carbon chain length of the SFA increased.[13] However, our obtained results were not consistent with these conclusions. The films with AA (C20:0) and LA (C12:0) showed lower WVP values than the films with SA (C18:0), PA (C16:0), and MA (C14:0). The results suggest that the presence of SFAs influenced the WVP more than the hydrophobicity carbon chain length, but other factors were also present.

CONCLUSIONS

The SFAs caused a decrease in the PV and BD values of the SPS and significantly changed other feature point viscosity values. The addition of SFA lowered the MW values of amylose. The SFAs had significant effects on the properties of the SPS–SFA composite films. The films with SFA showed a continuous and uniform structure compared to the SFA-free film. The SPS–SFA composite films showed higher TSs and better barrier properties to water vapor than the control films. For the films with SFAs, the T_o and T_p values increased. The SPS–SFA polymer matrix had a lower E and light transmission compared with the control films.

In short, SPS could be used to produce biopolymer films with good properties. The addition of SFAs could improve the properties of these films. These films have great potentiality for use as inner packaging in the food industry; this could reduce the use of synthetic plastics and provide a positive environmental impact. However, the effect mechanism of SFA on the mechanical and WVP properties of the films was not clear and needs to be investigated further.

ACKNOWLEDGMENTS

The authors acknowledge the financial support from the Planning Subject of "the twelfth five-year" in National Science and Technology for the Rural Development of China (2013BAD18B10-3).

REFERENCES

1. Maizura, M.; Fazilah, A.; Norziah, M. H.; Karim, A. A. *J. Food Sci. C* **2007**, *72*, 324.
2. Mali, S.; Grossmann, M. V. E.; Garcia, M. A.; Martino, M. N.; Zaritzky, N. E. *Food Hydrocolloids* **2005**, *19*, 157.
3. Shen, X. L.; Wu, J. M.; Chen, Y. H.; Zhao, G. H. *Food Hydrocolloids* **2010**, *24*, 285.
4. Liu, W. *Chin. Agric. Sci. Bull.* **2007**, *23*, 484.
5. Gareia, M. A.; Martino, M. N.; Zaritzky, N. E. *Scanning* **1999**, *21*, 348.
6. Vorwerg, W.; Dijksterhuis, J.; Borghuis, J. *Starch* **2004**, *56*, 297.
7. Mali, S.; Sakanaka, L. S.; Yamashita, F.; Grossmann, M. V. E. *Carbohydr. Polym.* **2005**, *60*, 283.
8. Fringant, C.; Rinaudo, M.; Bardet, B. *Carbohydr. Polym.* **1998**, *35*, 97.
9. Zahedi, Y.; Ghanbarzadeh, B.; Sedaghat, N. *J. Food Eng.* **2010**, *100*, 102.
10. Gontard, N.; Marchesseau, S.; Cuq, J. L.; Guilbert, S. *Int. J. Food Sci. Technol.* **1995**, *30*, 49.
11. Fernández, L.; Díaz de Apodaca, E.; Cebrían, M.; Villarán, M. C.; Maté, J. I. *Eur. Food Res. Technol.* **2007**, *224*, 415.
12. Fabra, M. J.; Jiménez, A.; Atarés, L.; Talens, P.; Chiralt, A. *Biomacromolecules* **2009**, *10*, 1500.
13. Jiménez, A.; Fabra, M. J.; Talens, P.; Chiralt, A. *Carbohydr. Polym.* **2010**, *82*, 585.
14. Ross, A. S.; Walker, C. E.; Booth, R. I.; Orth, R. A.; Wrigley, C. W. *Cereal Foods World* **1987**, *32*, 827.
15. American Society for Testing and Materials. In Annual Book of ASTM Standards; ASTM D 882-02; American Society for Testing and Materials: Philadelphia, PA, 2002.
16. Tang, X. Z.; Alavi, S.; Herald, T. *J. Carbohydr. Polym.* **2008**, *74*, 552.
17. Yan, Q. Q.; Hou, H. X.; Guo, P.; Dong, H. Z. *Carbohydr. Polym.* **2012**, *87*, 707.
18. Gao, W.; Dong, H. Z.; Hou, H. X.; Zhang, H. *Carbohydr. Polym.* **2012**, *88*, 321.
19. Zhou, Z. K.; Robards, K.; Helliwell, S.; Blanchard, C. *Food Res. Int.* **2007**, *40*, 209.
20. Kim, C. S.; Walker, C. E. *J. Food Sci.* **1992**, *57*, 1009.
21. Tang, M. C.; Copeland, L. *Carbohydr. Polym.* **2007**, *67*, 80.
22. Raphaelides, S. N.; Georgiadis, N. *Carbohydr. Polym.* **2006**, *65*, 81.
23. Nobrega, M. M.; Olivato, J. B.; Grossmann, M. V. E.; Bona, E.; Yamashita, F. *J. Appl. Polym. Sci.* **2011**, *124*, 3695.
24. Kaur, K.; Singh, N. *Food Chem.* **2000**, *71*, 511.
25. Morrison, W. R.; Law, R. V.; Snape, C. E. *J. Cereal Sci.* **1993**, *18*, 107.
26. Raphaelides, S. N.; Dimitreli, G.; Exarhopoulos, S.; Mintzas, D.; Lykidou, A. *Carbohydr. Polym.* **2012**, *88*, 282.
27. Godet, M. C.; Tran, V.; Delagw, M. M. *Int. J. Biol. Macromol.* **1993**, *15*, 11.
28. Whistler, R. L. Methods in Carbohydrate Chemistry; Academic: New York, **1964**.
29. Nebesny, E.; Kwasniewska-Karolak, I.; Rosicka-Kaczmarek, J. *Starch* **2005**, *57*, 378.
30. Raphaelides, S. N.; Georgiadis, N. *Food Hydrocolloids* **2007**, *21*, 1188.
31. Exarhopoulos, S.; Raphaelides, S. N. *J. Cereal Sci.* **2012**, *55*, 139.
32. Schmidt, V. C. R.; Porto, L. M.; Laurindoa, J. B.; Menegalli, F. C. *Ind. Crops Prod.* **2013**, *41*, 227.
33. Shellhammer, T. H.; Krochta, J. M. *J. Food Sci.* **1997**, *62*, 390.

34. Tanner, K. E.; Getz, J. J.; Burnett, S.; Youngblood, E.; Draper, P. R. U.S. Pat. 6-582-727 (**2003**).

35. Fabra, M. J.; Talens, P.; Chiralt, A. *J. Food Eng.* **2010**, *96*, 356.

36. Villalobos, R.; Chanona, J.; Hernández, P.; Gutiérrez, G.; Chiralt, A. *Food Hydrocolloids* **2005**, *19*, 53.

37. Fakhouri, F. M.; Batista, J. A.; Grosso, C. R. F. *Braz. J. Food Technol.* **2003**, *6*, 301.

38. Fakhouri, F. M.; Fontes, L. C. B.; Innocentini-Mei, L. H.; Collares-Queiroz, F. P. *Starch* **2009**, *61*, 528.

39. Ayranci, E.; Tunc, S. *Food Chem.* **2001**, *72*, 231.

40. Sanchez, G. L.; Vargas, M.; Gonzalez, M. C.; Chiralt, A.; Chafer, M. *Food Hydrocolloids* **2009**, *23*, 2102.

41. Lai, H. M.; Padua, G. W.; Wei, L. S. *Cereal Chem.* **1997**, *74*, 49.

42. Pascat, B. In Food Packaging and Preservation: Theory and Practice; Mathlouthi, M., Ed.; Elsevier Applied Science: London, **1986**; p 7.

43. McHugh, T. H.; Krochta, J. M. *J. Am. Oil Chem. Soc.* **1994**, *71*, 307.

44. Tanaka, M.; Ishizaki, S.; Suzuki, T.; Takai, R. *J. Tokyo Univ. Fisheries* **2001**, *87*, 31.